Am. J. Hum. Genet. 76:112–127, 2005

Extreme Heterogeneity in the Molecular Events Leading to the Establishment of Chiasmata during Meiosis I in Human Oocytes

Michelle L. Lenzi,[1] Jenetta Smith,[1] Timothy Snowden,[4] Mimi Kim,[2] Richard Fishel,[4] Bradford K. Poulos,[3] and Paula E. Cohen[1,*]

Departments of [1]Molecular Genetics, [2]Epidemiology and Population Health, and [3]Pathology, Albert Einstein College of Medicine, Bronx, NY; and [4]Kimmel Cancer Center, Philadelphia

In humans, ~50% of conceptuses are chromosomally aneuploid as a consequence of errors in meiosis, and most of these aneuploid conceptuses result in spontaneous miscarriage. Of these aneuploidy events, 70% originate during maternal meiosis, with the majority proposed to arise as a direct result of defective crossing over during meiotic recombination in prophase I. By contrast, <1%–2% of mouse germ cells exhibit prophase I–related nondisjunction events. This disparity among mammalian species is surprising, given the conservation of genes and events that regulate meiotic progression. To understand the mechanisms that might be responsible for the high error rates seen in human females, we sought to further elucidate the regulation of meiotic prophase I at the molecular cytogenetic level. Given that these events occur during embryonic development in females, samples were obtained during a defined period of gestation (17–24 weeks). Here, we demonstrate that human oocytes enter meiotic prophase I and progress through early recombination events in a similar temporal framework to mice. However, at pachynema, when chromosomes are fully paired, we find significant heterogeneity in the localization of the MutL homologs, MLH1 and MLH3, among human oocyte populations. MLH1 and MLH3 have been shown to mark late-meiotic nodules that correlate well with—and are thought to give rise to—the sites of reciprocal recombination between homologous chromosomes, which suggests a possible 10-fold variation in the processing of nascent recombination events. If such variability persists through development and into adulthood, these data would suggest that as many as 30% of human oocytes are predisposed to aneuploidy as a result of prophase I defects in MutL homolog–related events.

Introduction

Meiotic recombination ensures correct disjunction of chromosomes to provide haploid germ cells for fertilization and is dependent on both (1) the correct alignment of—and the physical connection between—homologous maternal and paternal chromosomes and (2) the appropriate reciprocal recombination between opposing homologs. Both the frequency and the placement of crossovers (chiasmata) are essential for correct segregation. Underlying these processes is the formation of the synaptonemal complex (SC), a proteinaceous structure that is the hallmark feature of meiotic prophase I. The SC consists of axial elements that align each homolog and a central element that tethers homologs together until the maturation of the chiasmata. The fact that SC formation, homolog pairing, and recombination are intricately linked is demonstrated by the observation that disruption of one event, such as SC formation, has severe consequences for the other events. For example, mice harboring mutations in the gene encoding a key SC protein, Sycp3 (MIM 604759), exhibit male sterility due to apoptotic loss of germ cells during prophase I prior to synapsis and display altered distribution of proteins involved in recombination (Yuan et al. 2000, 2002). Interestingly, in *Sycp3*$^{-/-}$ females, mature oocytes can be obtained but are severely aneuploid. Thus, oocytes survive longer than spermatocytes in *Sycp3*$^{-/-}$ mice, although the requirement for SYCP3 in chiasma formation and in the maintenance of chromosomal integrity eventually results in failure of chromosome segregation (Yuan et al. 2002).

The molecular events regulating recombination and meiotic progression in mice have been the subject of much recent interest and investigation (reviewed by Bannister and Schimenti [2004]). Recombination in most sexually reproducing species is instigated by an SPO11-dependent double-stranded break (DSB) (Keeney et al. 1997) that is processed initially by single-stranded binding proteins that include RAD51 (MIM 179617) and replication protein A (RPA [MIM 179835, MIM 179836, and MIM

Received September 28, 2004; accepted for publication November 8, 2004; electronically published November 22, 2004.

Address for correspondence and reprints: Dr. Paula E. Cohen, Cornell University, Department of Biomedical Sciences, T3 014, Veterinary Research Tower, Ithaca, NY 14853. E-mail: pc242@cornell.edu

* Present affiliation: Department of Biomedical Sciences, Cornell University, Ithaca, NY.

0002-9297/2005/7601-0011$15.00

179837]). The initial product is a progenitor Holliday-junction recombination intermediate that appears to be stabilized by the meiosis-specific MutS homologs, MSH4 and MSH5 (MIM 602105 and MIM 603382, respectively), which form sliding clamps that embrace homologous chromosomes (Ross-Macdonald and Roeder 1994; Hollingsworth et al. 1995; Snowden et al. 2004). These MutS homologs are members of the DNA mismatch repair (MMR) family but do not appear to function in classic MMR processes (reviewed by Hoffmann and Borts [2004]). Instead, the MSH4-MSH5 heterodimer is essential for reciprocal recombination events in *Saccharomyces cerevisiae* (Winand et al. 1998; Hoffmann and Borts 2004), *Caenorhabditis elegans* (Zalevsky et al. 1999; Kelly et al. 2000), *Mus musculus* (de Vries et al. 1999; Edelmann et al. 1999; Kneitz et al. 2000), and *Arabidopsis thaliana* (Higgins et al. 2004).

In mice and yeast, a fraction of the MSH4-MSH5–positive recombination intermediates are subsequently processed to form double Holliday junctions (dHJs) that are the consensus crossover structures associated with the chiasmata that ultimately ensure accurate chromosome disjunction (Allers and Lichten 2001). The selection of these dHJ sites is effected by the accumulation of the MutL homologs, MLH1 and MLH3 (MIM 120436 and MIM 604395, respectively), at a subset of these structures (Baker et al. 1996; Hunter and Borts 1997; Wang et al. 1999; Lipkin et al. 2002; Hoffmann et al. 2003; Hoffmann and Borts 2004). MLH1 and MLH3 are also members of the MMR family, and they appear to function, in heterodimeric form, in both meiotic recombination and canonical repair events. MLH1-MLH3 heterodimers promote crossing over in an MSH4-MSH5–dependent manner (Wang et al. 1999; Borts et al. 2000; Abdullah et al. 2004) and are essential for normal meiotic progression in both yeast and mice (reviewed by Kolas and Cohen [2004]). Moreover, MLH1 and MLH3 are now recognized to be molecular markers of late-meiotic (or recombination) nodules during pachynema of prophase I in mice and humans (Lynn et al. 2004), and these nodule structures are thought to give rise to the mature crossover structures that appear at diplonema (Marcon and Moens 2003).

Comparison of meiotic events in yeast, worms, and mice has revealed that these genes and molecular events are highly conserved (Zalevsky et al. 1999; Moens et al. 2002; Kolas and Cohen 2004), which leads us to question whether the same holds true for human meiosis. Few studies have been performed in human male germ cells (Barlow and Hulten 1998; Hassold et al. 2004; Lynn et al. 2004), and even fewer studies have been performed in human female germ cells (Tease et al. 2002; Roig et al. 2004); all of these studies indicate that MLH1 is present at late-meiotic nodules in human germ cells. However, these studies have not explored the dynamic progression of prophase I events in human germ cells, in part because of the limited availability of such tissue. Given the high error rate seen in human meiotic products, particularly in oocytes, we hypothesize that disruption of the molecular events surrounding recombination in female germ cells might be, in part, responsible for the high rate of nondisjunction seen in human conceptuses. Indeed, studies in the mouse, such as in *Sycp3*$^{-/-}$ animals (Yuan et al. 2000, 2002), indicate that there are major differences in the efficiency of male and female meiosis, in that mutations that disrupt meiosis in males result in apoptotic elimination of spermatocytes, whereas the same mutation in females usually results in the progression of defective oocytes to meiosis II. To extend such studies to humans, the present study was aimed at exploring the temporal regulation of prophase I events in human fetal oocytes, with special emphasis on the initiation and progression of recombination. Our studies demonstrate that human fetal oocytes are extremely heterogeneous with respect to the ultimate selection of crossover events and that this variability occurs at the level of the stabilization of MSH4-MSH5–positive sites by members of the MutL-homolog family.

Material and Methods

Tissue

Human fetal ovaries were obtained from the Albert Einstein College of Medicine Human Fetal Tissue Repository, in accordance with institutional review board regulations. Fetal tissue was acquired from women (mean maternal age 24.9 ± 6.5 years) undergoing elective pregnancy terminations between 17 and 24 wk of gestation (mean gestational age 21.5 ± 1.8 wk). Pairs of ovaries were maintained in 50 ml of Dulbecco's modified Eagle medium and were obtained within 1 h of retrieval.

Meiotic Preparations

Chromosome "spreads" were prepared from human fetal oocytes by use of the drying-down technique described by Peters et al. (1997), with modifications. Ovaries were trimmed of extraneous tissue and then rinsed with PBS (pH 7.4). Each ovary was immersed in hypotonic extraction buffer (pH 8.2) (30 mM Tris [pH 8.2], 50 mM sucrose, 17 mM trisodium citrate, 5 mM EDTA, 0.5 mM DTT, and 0.5 mM PMSF) and was placed on ice for 1 h. Each ovary was sectioned in half, and one half was stored on ice while the other was minced in 75 μL 100 mM sucrose (pH 8.2). A 6 × 8 mm well slide was dipped quickly in 1% paraformaldehyde (PFA) containing 0.15% Triton X-100 (pH 9.2). The cell slurry was returned to ice while the other ovary half was minced. The bottom righthand corner of the

slide was blotted with a paper towel, leaving PFA primarily over the surface of the wells. To each well, 2 μl of the oocyte slurry were added to the upper righthand corner. The slide was tilted diagonally to allow the chromosomes to spread evenly over the well. For each ovary, four six-well slides were prepared. Slides were immediately placed in a sealed humidity chamber and were left overnight. The next morning, the slides were rinsed three times in 0.4% Photo-Flo (Kodak) for 2 min and were allowed to air-dry. Slides not used immediately were stored at −80°C, and the others were prepared for chromosome immunofluorescence by use of procedures described elsewhere (Lipkin et al. 2002).

Antibodies

Polyclonal mouse and rabbit antibodies against the SC protein, SYCP3, were used to identify meiotic cells. These antibodies were generated from full-length SYCP3 His(6x)-tagged protein expressed in bacteria, were purified through a nickel column (Ni-NTA agarose [Qiagen]), and then either were used to immunize mice in-house or were sent to Covance laboratories for generation of rabbit antibodies. Mouse and rabbit anti–phospho-histone H2AX (MIM 601772) (Ser139 [Upstate Cell Signaling Solutions]) antibodies were used to detect the presence of DSBs. Rabbit polyclonal antibody against the human RAD51 protein (Ab-1 [Oncogene]) was used to detect early meiotic nodules, which are complexes associated with the SC. Late-meiotic nodules were identified using the rabbit polyclonal antibody against RPA (a gift from Peter Moens, York University, Toronto). Affinity-purified rabbit antisera against MSH4 and MSH5 were used to identify these proteins along the SC. Monoclonal anti-human MLH1 (BD Pharmingen) and polyclonal rabbit anti-MLH3 (Lipkin et al. 2002) served to visualize crossover sites. Centromeres were identified using human serum from patients with CREST (calcinosis, Raynaud's, esophagus, sclerodactyly, telangiectasia).

Chromosome Analysis

Images were captured on an Olympus Provis microscope by use of IPLab imaging software; they were then compiled using Adobe Photoshop. Each oocyte nucleus was staged according to SC appearance, degree of synapsis, and molecular markers for prophase I. Data were tabulated and analyzed using Prism 4.0 software.

Chromosome Staging

Oocyte nuclei were staged according to the number of centromeric signals (illuminated by CREST), the degree of formation of the SC (illuminated by SYCP3), and the thickness of the synapsed homologous chromosome cores. Leptotene nuclei were identified by 46 centromeric signals, an indication that synapsis has not yet occurred. Components of the SC were visible as a few scattered foci. Zygotene cells had between 23 and 45 centromeres. The SCs of zygotene nuclei were more distinct than those of nuclei in leptonema. Early zygotene cells had between 34 and 45 centromeres. The SCs were visible as many discrete foci throughout the nucleus. In late-zygotene cells, the SCs appeared as stringlike structures, with 24 to 33 centromeric signals. Nuclei of pachytene oocytes had 23 centromeric signals. The degree of intensity, the length, and the thickness of the synapsed chromosome cores were used to determine whether the nucleus was in early, middle, or late pachynema. Nuclei in early pachynema had SCs that were longer, more faint, and less compacted than those in mid- and late-pachynema nuclei. In mid-pachytene oocyte nuclei, SCs were shorter, brighter and denser than those in early-pachytene nuclei. Late-pachytene nuclei had the shortest, brightest, and densest SCs. Diplotene nuclei had 23 centromeric signals, but the SCs showed signs of desynapsis, looping and rejoining at sites of chiasmata.

Calculation of Interference Parameter

Distances between MLH1 intervals were computed, and a two-parameter gamma distribution was fitted to the data by use of the maximum-likelihood method. On each chromosome, the distance from the final MLH1 focus to the telomere was treated as a right-censored observation, as in the study by Broman and Weber (2000). The shape parameter in the gamma distribution, ν, measures the strength of interference, where $\nu = 1$ corresponds to no interference, $\nu > 1$ corresponds to positive interference, and $\nu < 1$ indicates negative interference. CIs for ν were based on the profile-likelihood approach.

Results

Accumulation and Persistence of DSBs, as Assessed by Localization of Phosphorylated H2AX, in Prophase I

The presence of meiotic DSBs may be visualized with antibodies against the phosphorylated form of the core histone H2AX, known as "γH2AX," which accumulates at DSB sites early in leptonema in mouse germ cells (Mahadevaiah et al. 2001). Although the human *SPO11* gene (MIM 605114) has been cloned (Romanienko and Camerini-Otero 1999) and the appearance of γH2AX has been described in human spermatocytes (Judis et al. 2004), no information is available concerning the status of γH2AX in human oocytes during prophase I, nor regarding the temporal dynamics of γH2AX in human germ cells in general. Fluorescent antibodies to the SC protein, SYCP3, localize to and visually define the axial elements (AEs) of the developing SC prior to synapsis (green signal in fig. 1). γH2AX colocalizes with SYCP3 on human oocyte chromosomes in early leptonema as

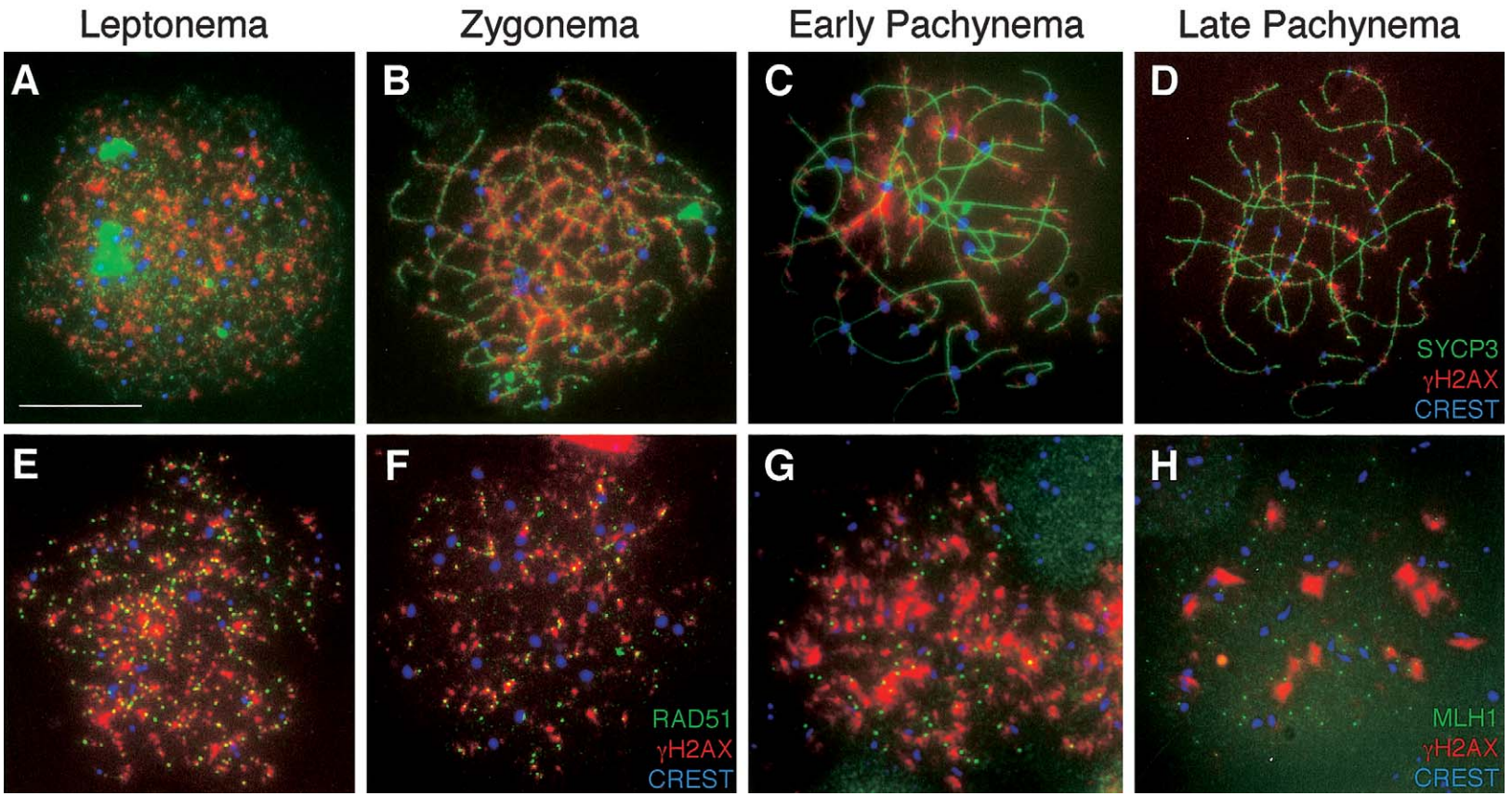

Figure 1 Localization of γH2AX during prophase I in human fetal oocytes. *A–D,* γH2AX localizes to human female meiotic chromosomes during each substage of prophase I. Human oocyte chromosome "spreads" were subjected to immunofluorescent localization of SYCP3, a component of the SC (*green,* FITC), with γH2AX (*red,* TRITC) and CREST (*blue,* Cy5), at leptonema (*A*), zygonema (*B*), early pachynema (*C*), and late pachynema (*D*). In addition, γH2AX (*red,* TRITC) was colocalized with sites containing either RAD51 (*E* and *F*) or MLH1 (*G* and *H*). In panels E, F, G, and H, γH2AX (*red,* TRITC) is colocalized with RAD51 (*green,* FITC) and CREST (*blue,* Cy5) during leptonema (*E*) and zygonema (*F*). In panels G and H, γH2AX (*red,* TRITC) is colocalized with MLH1 (*green,* FITC) and CREST (*blue*, Cy5) during late zygonema (*G*) and pachynema (*H*). Scale bar = 10 μm.

the AE forms (fig. 1*A*), becoming more focal as the AEs become more clearly defined in zygonema (fig. 1*B*). This localization persists at a subset of sites, even into late pachynema (fig. 1*C* and 1*D*), at which time all DSB sites should have been repaired or processed further along homologous recombination pathways. In contrast, in the mouse, γH2AX localization occurs in large domains prior to synapsis at leptonema and persists through zygonema, when it associates predominantly with sites that have yet to synapse (Mahadevaiah et al. 2001). By late zygonema, much of the γH2AX is lost from the autosomes in mouse spermatocytes and localizes predominantly in the sex body (Mahadevaiah et al. 2001). Thus, a major difference between DSB processing during meiosis in human females and that in male mice is the increased and persistent γH2AX signal through pachynema. These later γH2AX sites could represent new DSBs that have yet to be processed by recombination machinery, or they could be the result of some other alteration within the chromatin architecture that results from SPO11-independent damage (Hamer et al. 2003). Alternatively, the persistent γH2AX signal could also be the result of a failure to properly dephosphorylate the histone after break repair, or it could suggest that the dynamics of H2AX phosphorylation/dephosphorylation are different in human germ cells, compared with those reported elsewhere for mouse germ cells.

DSB Processing by Single-Stranded Binding Proteins RPA and RAD51 in Human Fetal Oocytes

To examine the processing of DSB events, we employed a range of markers specific to individual events in the multistep formation of dHJs. The RecA homolog, RAD51, assembles helical nucleoprotein filaments on 3′ resected DNA ends after DSB induction (Bishop 1994) and associates with AEs prior to synapsis in leptonema until late zygonema in mouse and human spermatocytes (Ashley et al. 1995; Plug et al. 1996; Barlow et al. 1997; Cohen and Pollard 2001). In human fetal oocytes, RAD51 accumulates on AEs from early leptonema (figs. 2*A* and 3*A*), when it associates almost exclusively with γH2AX-positive regions of the genome (fig. 1*E* and 1*F*). More than 300 RAD51 foci remain until zygonema, similar to the frequency of γH2AX distribution along synapsing chromosome cores. Unlike mouse spermatocytes, human RAD51 remains associated with oocyte chromosomes through synapsis, with high numbers of RAD51-positive foci persisting until early pachynema (fig. 2*A* and fig. 3*B* and 3*C*). By late pachynema (fig. 3*D*), the number of RAD51 foci has declined to about half of that found in leptonema. The number of residual RAD51 foci declines further by the end of pachynema, and the foci most likely represent the late γH2AX events that have either failed to be processed or that are induced later during prophase I. Interestingly, by late pachynema, the numbers of RAD51 foci and γH2AX foci are not statistically different (49.5 ± 19.0 and 35.6 ± 18.1, respectively [$P = .13$]), which suggests that all γH2AX sites are targeted by RAD51, even at this late stage.

RPA is a heterotrimeric protein complex that consists of 14-, 32-, and 70-kDa subunits, the latter of which bind directly to single-stranded DNA to effect functions in DNA replication, repair, and recombination. During mouse meiosis, RPA associates with chromosome cores of synapsing homologs and appears to marginally overlap with the localization profile of RAD51 (Plug et al. 1998). RAD51 disappears from AEs by early pachynema in mouse spermatocytes, whereas RPA persists and then declines steadily through this stage. In human oocytes, we observe a similar temporal localization profile (figs. 2*B* and 3*E*), with RPA foci being observed in persistently high numbers from leptonema through early pachynema. Thereafter, the number of RPA foci drops dramatically at mid-pachynema to <10% of the early–prophase I levels, and most foci are gone by late pachynema (fig. 3*F*–3*H*).

Appearance of MutS Homologs Define a Substage of Recombination Intermediate Selection

MSH4 and MSH5 form a heterodimer (Bocker et al. 1999) that is essential for meiotic recombination events in yeast (Ross-Macdonald and Roeder 1994; Hollingsworth et al. 1995), worms (Zalevsky et al. 1999), and mice (de Vries et al. 1999; Edelmann et al. 1999; Kneitz et al. 2000). In yeast, the MSH4-MSH5 heterodimer has been implicated in chromosome synapsis, crossover selection, and resolution (Hollingsworth et al. 1995; Novak et al. 2001), whereas, in mice, this heterodimer is thought to interact in early prophase I with RAD51-positive meiotic nodules (P.E.C., unpublished observations). Thus, mutation of either *Msh4* or *Msh5* in mice results in sterility due to synaptic failure during late zygonema (de Vries et al. 1999; Edelmann et al. 1999; Kneitz et al. 2000). The MSH4-MSH5 heterodimer has been shown to recognize and bind to pro-HJs and dHJs in vitro (Bocker et al. 1999; Snowden et al. 2004), forming a sliding clamp that appears to stabilize recombination intermediates and ultimately promotes crossing over. As in mouse spermatocytes, MSH4 localizes throughout the nucleus of human oocytes from leptonema (figs. 2*C* and 4*A*) but does not associate with SYCP3 until zygonema (fig. 4*B*), when both MSH4 and MSH5 localize to discrete foci at a frequency of 44%–58% of that seen for RAD51 (fig. 2*C* and 2*D* and fig. 4*A*, 4*B*, 4*E*, and 4*F*). Their localization initially occurs on asynapsed cores and increases by late zygonema to ~70% of RAD51 numbers, after which time they decline through late pachynema (fig. 4*C*, 4*D*, 4*G*, and 4*H*). This localization demonstrates, for the first time, that MSH5 colocalizes on SCs with MSH4 in mammalian

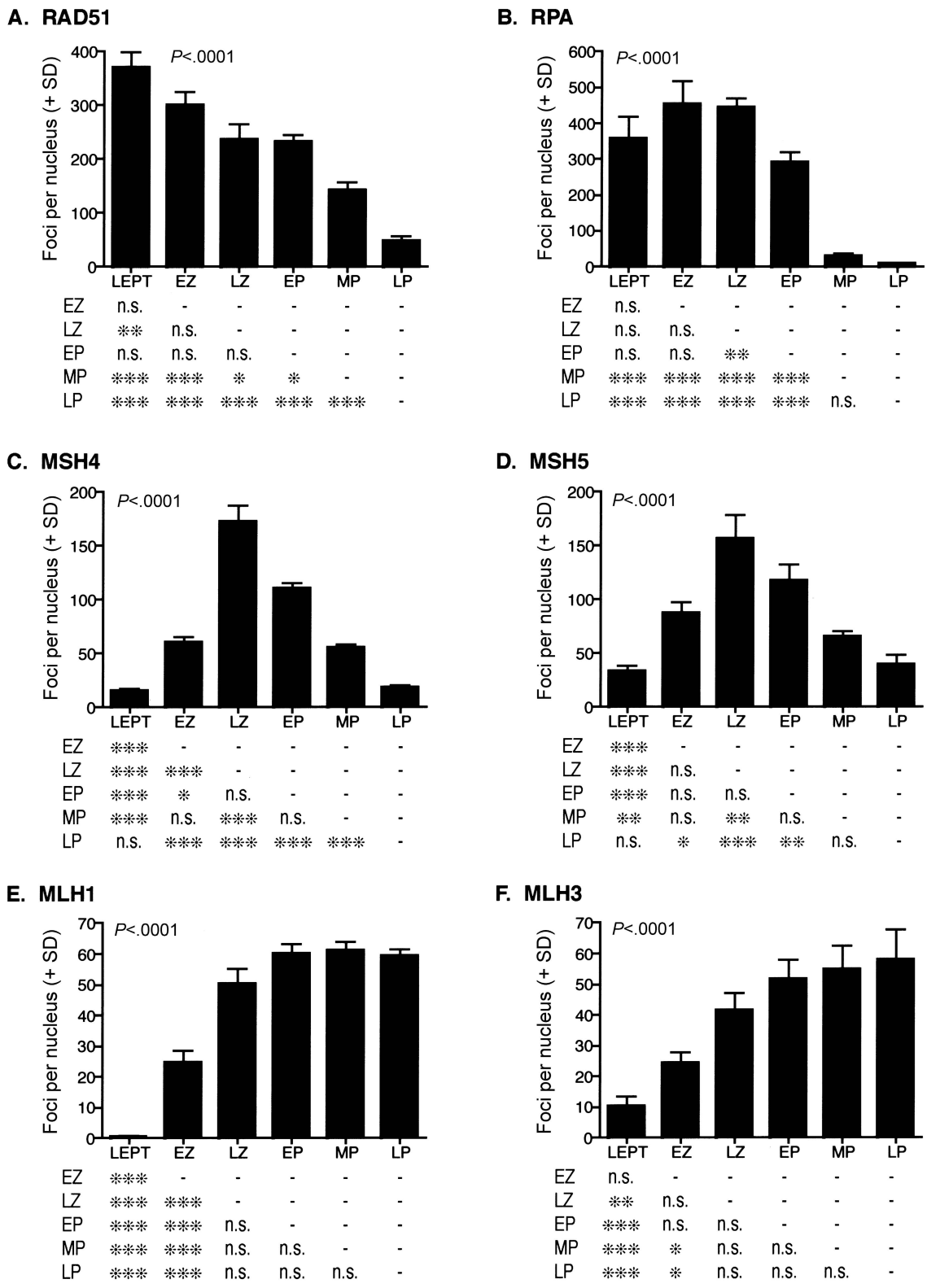

Figure 2 Localization of DNA repair proteins during prophase I in human fetal oocytes. Graphs show quantitation (number of foci per nucleus + SD) for each substage of prophase I for RAD51 (*A*), RPA (*B*), MSH4 (*C*), MSH5 (*D*), MLH1 (*E*), and MLH3 (*F*). Examples of these localization patterns are provided in figures 3–5. LEPT = leptonema; EZ = early zygonema; LZ = late zygonema; EP = early pachynema; MP = mid-pachynema; LP = late pachynema. Data were analyzed by ANOVA after log transformation to ensure equal variances (*P* values are given within each bar graph; in all cases, $P < .0001$). Pairwise comparisons of substages were performed using the Tukey posttest and are displayed in table format below each graph. One asterisk (*) indicates $P < .05$, two asterisks (**) indicate $P < .01$, and three asterisks (***) indicate $P < .001$; n.s. = not significant.

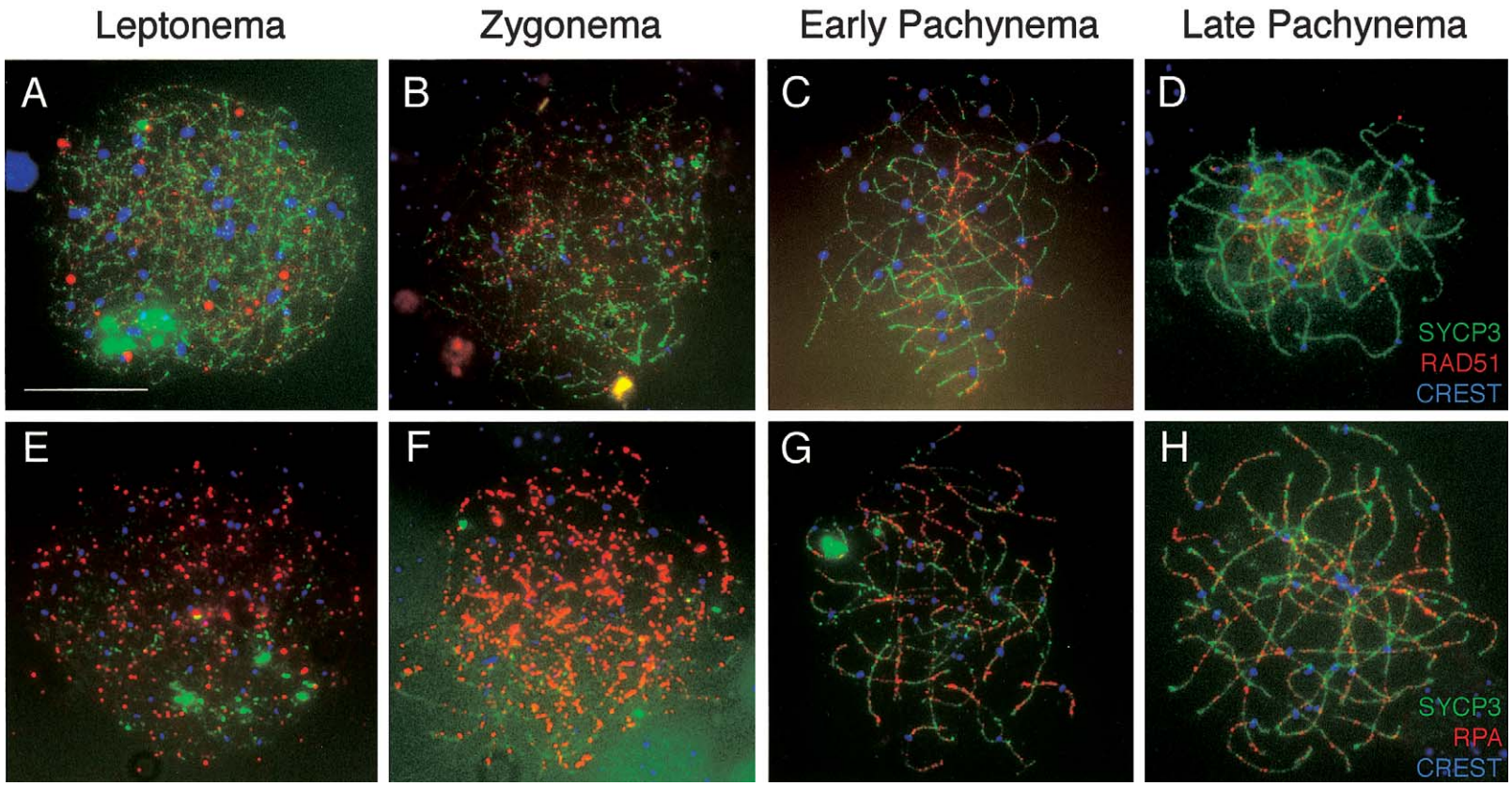

Figure 3 Localization of RAD51 and RPA during prophase I in human fetal oocytes. Human oocyte chromosome "spreads" were subjected to immunofluorescent localization of RAD51 and RPA to identify their pattern of distribution during each substage of prophase I. *A–D,* For each stage, RAD51 (*red,* TRITC) is shown with SYCP3 (*green,* FITC) and CREST (*blue,* Cy5). *A,* Leptonema; *B,* zygonema; *C,* early pachynema; and *D,* late pachynema. *E–H,* RPA (*red,* TRITC) is shown with SYCP3 (*green,* FITC) and CREST (*blue,* Cy5) during leptonema (*E*), zygonema (*F*), early pachynema (*G*), and late pachynema (*H*). Scale bar = 10 μm.

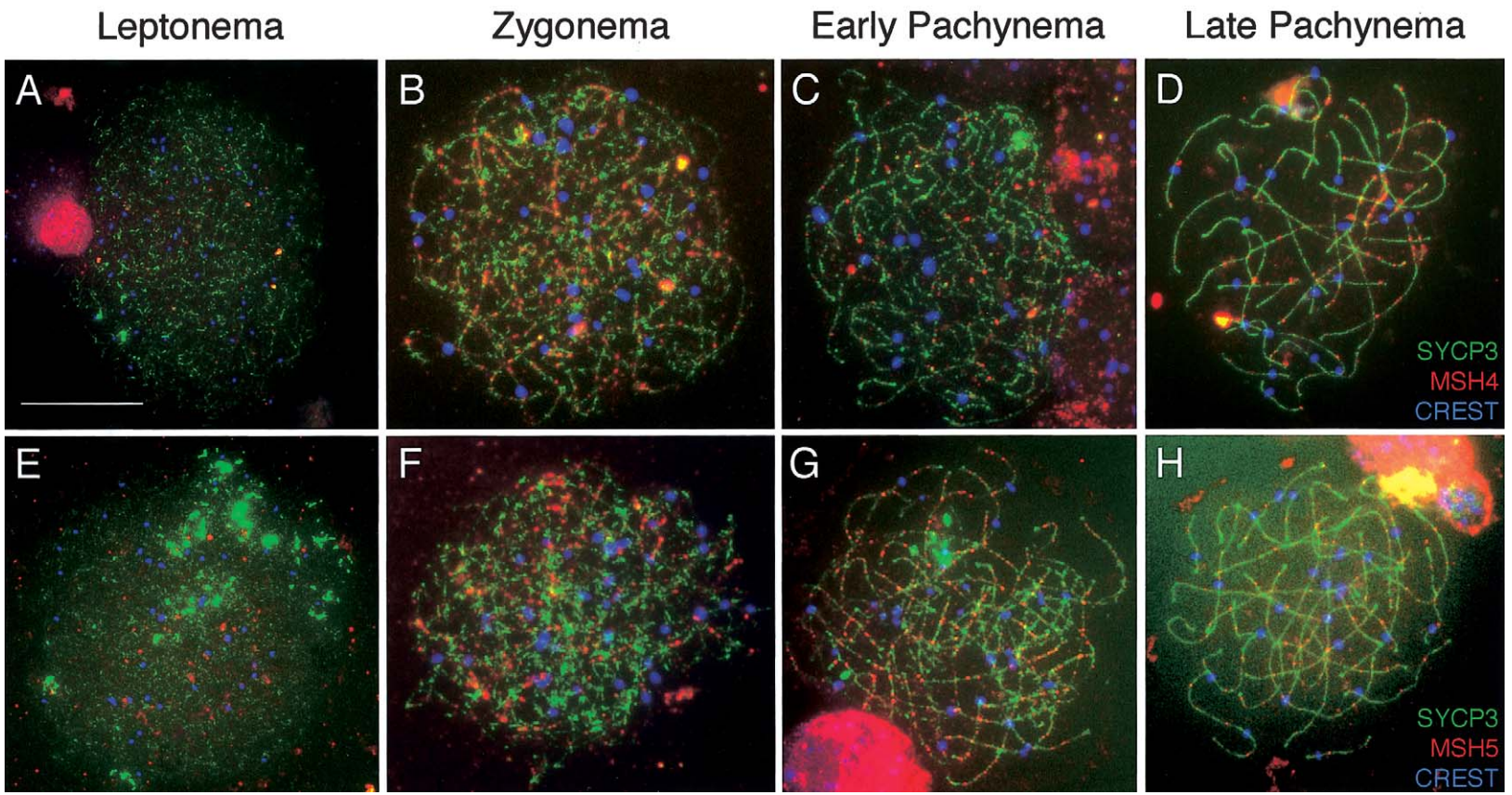

Figure 4 Localization of MSH4 and MSH5 during prophase I in human fetal oocytes. The MutS homologs, MSH4 and MSH5, are present along human female meiotic chromosomes during each substage of prophase I. *A–D,* During each stage, MSH4 (*red,* TRITC) is shown with SYCP3 (*green,* FITC) and CREST (*blue,* Cy5). *A,* Leptonema; *B,* zygonema; *C,* early pachynema; and *D,* late pachynema. MSH5 (*red,* TRITC) is shown with SYCP3 (*green,* FITC) and CREST (*blue,* Cy5) during leptonema (*E*), zygonema (*F*), early pachynema (*G*), and late pachynema (*H*). Scale bar = 10 μm.

germ cells at a time that would be predicted by the biochemical data (Snowden et al. 2004) and that correlates well with the murine models (Edelmann et al. 1999; Kneitz et al. 2000).

MutL-Homolog Association with Nascent Crossovers Reveals Large Heterogeneity in the Human Oocyte Population from Early Pachynema

The MutL homologs, MLH1 and MLH3, also function as a heterodimeric complex that has been proposed to associate with the MSH4-MSH5 heterodimer (Wang et al. 1999). In mouse spermatocytes, MLH1-MLH3 localizes to the late-meiotic nodules, the frequency of which is ~10-fold less than that of the initiating DSB events seen in leptonema (Cohen and Pollard 2001; Lipkin et al. 2002). Both *Mlh1*$^{-/-}$ and *Mlh3*$^{-/-}$ male and female mice are sterile as a result of a failure to process and/or maintain crossovers after SC breakdown, which results in premature desynapsis at or prior to metaphase (Baker et al. 1996; Woods et al. 1999; Lipkin et al. 2002). MLH1 has also been localized to presumptive sites of crossing over in human oocytes (Tease et al. 2002) and spermatocytes (Barlow and Hulten 1998; Judis et al. 2004), but, in both cases, the number of samples was extremely limited, precluding the ability to investigate MLH1 localization in any statistically quantitative fashion. Here, we used >15 samples from fetuses aged between 17 and 24 wk. More than 250 cells were analyzed at all stages of prophase I and were obtained within 1 h of surgery, reducing the risk of postmortem necrosis. We find that both MLH1 (fig. 2*E* and fig. 5*A*–5*D*) and MLH3 (fig. 2*F* and fig. 5*E*–5*H*) localize to synapsed meiotic chromosomes earlier in humans than in mice, accumulating in early zygonema and reaching a stable plateau upon synapsis at late zygonema (MLH1 and MLH3 focus numbers 50.3 ± 24.7 and 41.4 ± 26.5, respectively). In early zygonema, 65% of MLH1 foci colocalize with γH2AX, but, by late pachynema (fig. 1*G* and 1*H* and fig. 6), <7% of the total MLH1 foci that are present colocalize with γH2AX, which suggests that the majority of MLH1 is associated with repaired sites, presumably in conjunction with MSH4-MSH5.

Throughout pachynema, the number of MLH1-MLH3 foci are maintained (fig. 2*E* and 2*F* and fig. 5*C*, 5*D*, 5*G*, and 5*H*), but the variation of MLH1-MLH3 foci numbers is extremely high (n = 10–107) between oocytes, representing an ~10-fold variation in focus frequency. This variability is evident at the chromosome level as frequent achiasmate chromosome arms and whole chromosomes (fig. 5*I* and 5*J*) and chromosome arms that are overloaded with MLH1 foci (fig. 5*K* and 5*L*). By contrast, the number of MLH1 foci observed in mouse oocytes at this time is 27.5 ± 3.7, with a range of 20–33 (M. Lenzi, N. Kolas, and P. E. Cohen, unpublished observations). Thus, for human oocytes, the SD in MLH1-MLH3 focus numbers ranges from 24.5% to 53% through pachynema, whereas the SD for mouse values is significantly lower at 13% (Bartlett test $P < .0001$). A similar variation is not observed for MSH4 or MSH5 foci.

To investigate the dynamics of MLH1 variability on SCs from individual ovarian populations, we plotted the MLH1 focus counts for all oocytes, counted from individual embryos. Interestingly, as shown in figure 7, certain embryonic pools of oocytes exhibited a variation in MLH1 focus frequency that was much more severe than that in others, whereas some embryonic oocyte populations displayed significantly lower MLH1 frequencies than all other populations (arrows in fig. 7).

Discussion

The present study was aimed at establishing a time frame for the molecular events leading to chiasmata formation in human fetal oocytes. We used an array of cytological markers to visualize prophase I events in a statistically relevant sample population; our results serve both to highlight the similarities in meiotic recombination between mouse and human oocytes and, at the same time, to reveal distinct differences in the timing and efficiency of these events. First, we demonstrate that γH2AX-labeled DSBs are first seen prior to synapsis in human ovaries, which indicates the initiation of recombination events prior to physical homolog association, as in the mouse. The persistent localization of γH2AX on meiotic chromosome cores until diplonema indicates either that DSB repair has not been completed at these sites or that aberrant H2AX phosphorylation has occurred during the later stages of recombination. When DSB repair is completed in a temporally correct manner, the γH2AX signal should be lost by late zygonema. This notion is consistent with our demonstration that the percentage of MLH1 foci associated with γH2AX signal is high during zygonema but decreases steadily thereafter (fig. 6). Thus, the excessive γH2AX sites that are devoid of MLH1 at late pachynema—which reflect >96% of the total remaining γH2AX—might be the result of spontaneous DSBs or of other types of chromosome damage, or they might reflect later SPO11-induced events that have yet to acquire MLH1. If such cells were not subject to checkpoint elimination, this would result in a metaphase I oocyte in which DSBs were still apparent and that, presumably, either would result in apoptotic removal of the oocyte through checkpoint activation or would have a severe impact on the outcome of metaphase I progression. Alternatively, as mentioned above, it is possible that the persistent γH2AX signal represents sites that have yet to be dephosphorylated, an event that remains poorly characterized for meiotic cells. One final possibility is that DSB events are not strictly limited to

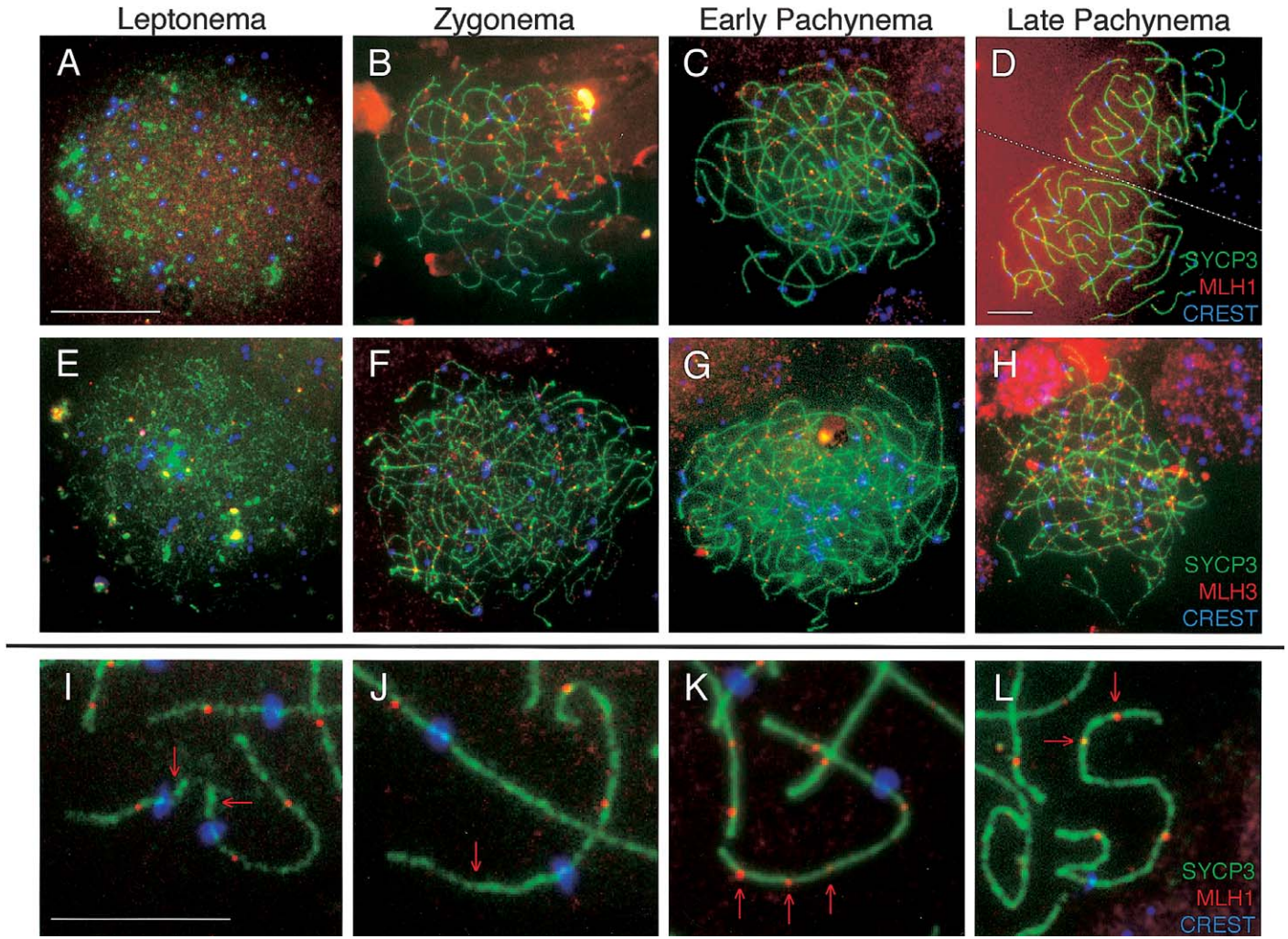

Figure 5 Localization of MLH1 and MLH3 during prophase I in human fetal oocytes. The MutL homologs, MLH1 and MLH3, localize to human female meiotic chromosomes during each substage of prophase I. *A–D,* MLH1 (*red,* TRITC) is shown with SYCP3 (*green,* FITC) and CREST (*blue,* Cy5) during leptonema (*A*), zygonema (*B*), early pachynema (*C*), and late pachynema (*D*). *E–H,* During each stage, MLH3 (*red,* TRITC) is shown with SYCP3 (*green,* FITC) and CREST (*blue,* Cy5). *E,* Leptonema; *F,* zygonema; *G,* early pachynema; and *H,* late pachynema. *I–L,* High magnification images of pachytene chromosomes highlights extreme variability in MLH1 localization, with some chromosome arms of pachytene oocytes often having too few MLH1 foci (arrows in *I* and *J*) or too many MLH1 foci (arrows in *K* and *L*). Green, SYCP3; red, MLH1; blue, CREST. Scale bar for panels A–C and E–H = 10 μm, scale bar for panel D = 10 μm, and scale bar for panels I–K = 5 μm. Note: at leptonema, γH2AX localization is almost continuous along the developing SC, so counts at this stage do not necessarily represent single foci.

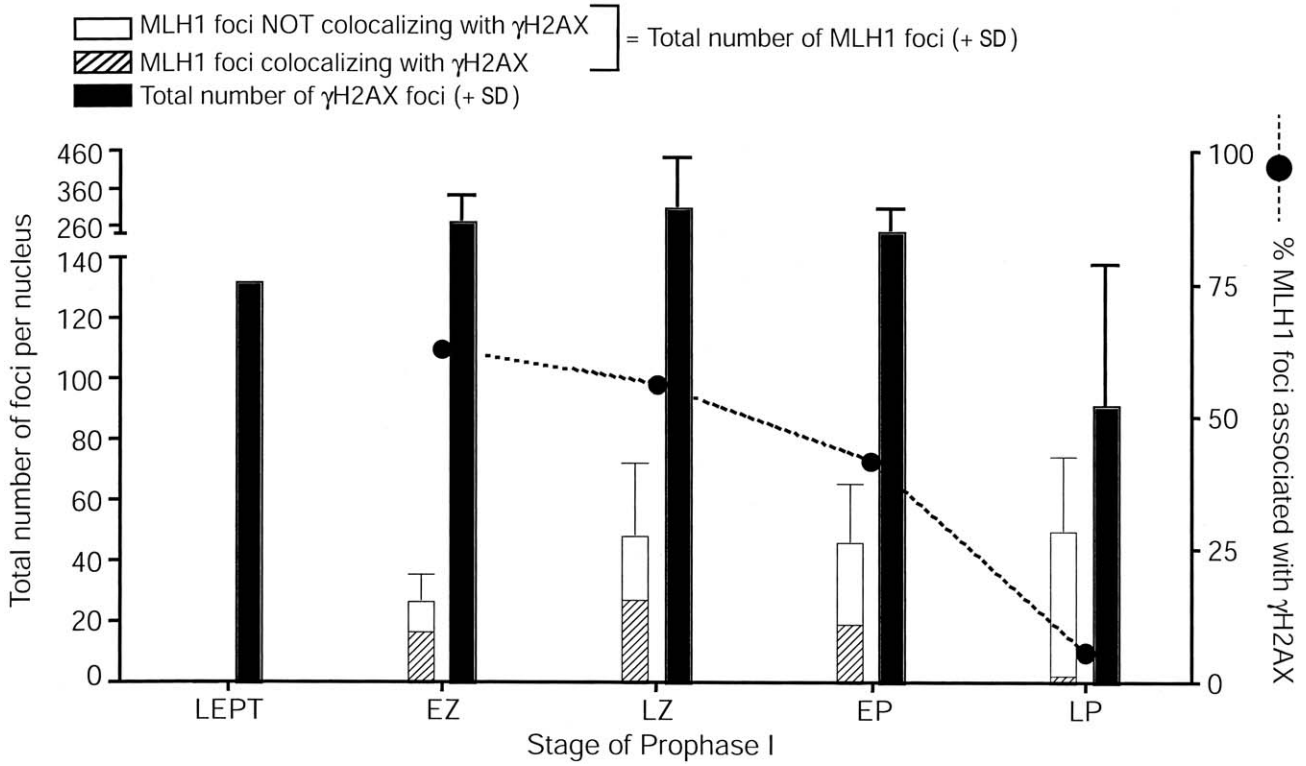

Figure 6 MLH1 interaction with γH2AX-positive sites throughout prophase I in human fetal oocytes. Colocalization of MLH1 with sites that contain γH2AX. For each stage, total MLH1 foci are shown in the left bar, which is subdivided into those MLH1 foci that are associated with γH2AX (*hatched portion of bar*) and those that are independent of γH2AX (*unhatched portion of bar*). The error bar reflects the SD for total MLH1 focus numbers. The blackened circles and dashed line represent the total percentage of MLH1 foci that are associated with γH2AX. The total number of γH2AX foci (+ SD) is represented by the right blackened bar for each stage.

leptonema in human oocytes and instead occur in successive waves throughout prophase I. Again, the impact of such a phenomenon on oocyte viability and chiasmata maintenance is unclear.

Recent studies by Roig et al. (2004) also examined the status of H2AX in human germ cells from both males and females ($n = 1$ and $n = 3$, respectively). Our findings for γH2AX localization are similar to those observed by Roig et al. (2004), showing persistent phosphorylation of H2AX and discrete focal patches of γH2AX at pachynema. Our observations, together with those of Roig et al. (2004), demonstrate that the γH2AX signal is not lost upon synapsis, as is seen in murine spermatocytes (Mahadevaiah et al. 2001). Furthermore, our observation that initial MLH1 foci in zygonema are associated with phospho-H2AX, whereas the residual phospho-H2AX in late pachynema is not associated with MLH1 (fig. 1*G* and 1*H* and fig. 6), suggests that later regions of phospho-H2AX are not associated with reciprocal recombination events at this time. These observations also suggest that the appearance of MLH1-MLH3 on meiotic chromosome cores might trigger the dephosphorylation of H2AX at reciprocal recombination sites, since the accumulation of MLH1-MLH3 is coupled with the localized loss of γH2AX signal.

We observed high variability in MLH1-MLH3 focus frequency during pachynema, which suggests that the selection of DSBs to become crossovers is inconsistent in human oocytes. Such variations in MLH1 frequency were alluded to by Tease et al. (2002) but were constrained by the small number of oocytes observed, by the fact that only three fetal ovary samples were used, and by the problems associated with extended delays between sample ascertainment and chromosome preparation. Nevertheless, these studies also demonstrated similar temporal dynamics for MLH1 appearance during prophase I and suggested a similarly variable frequency of foci during pachynema (Tease et al. 2002). Our present study extends the findings of the previous reports by revealing that MSH4-MSH5 focus numbers are more stable. Under the assumption that MLH1 and MLH3 are indicative of chiasmata sites, these results suggest that the crossover heterogeneity in human oocytes occurs at the level of MLH1-MLH3 targeting to MSH heterodimers, such that the MSH-MLH complex is not stabilized in a proportion of these cells. A stable

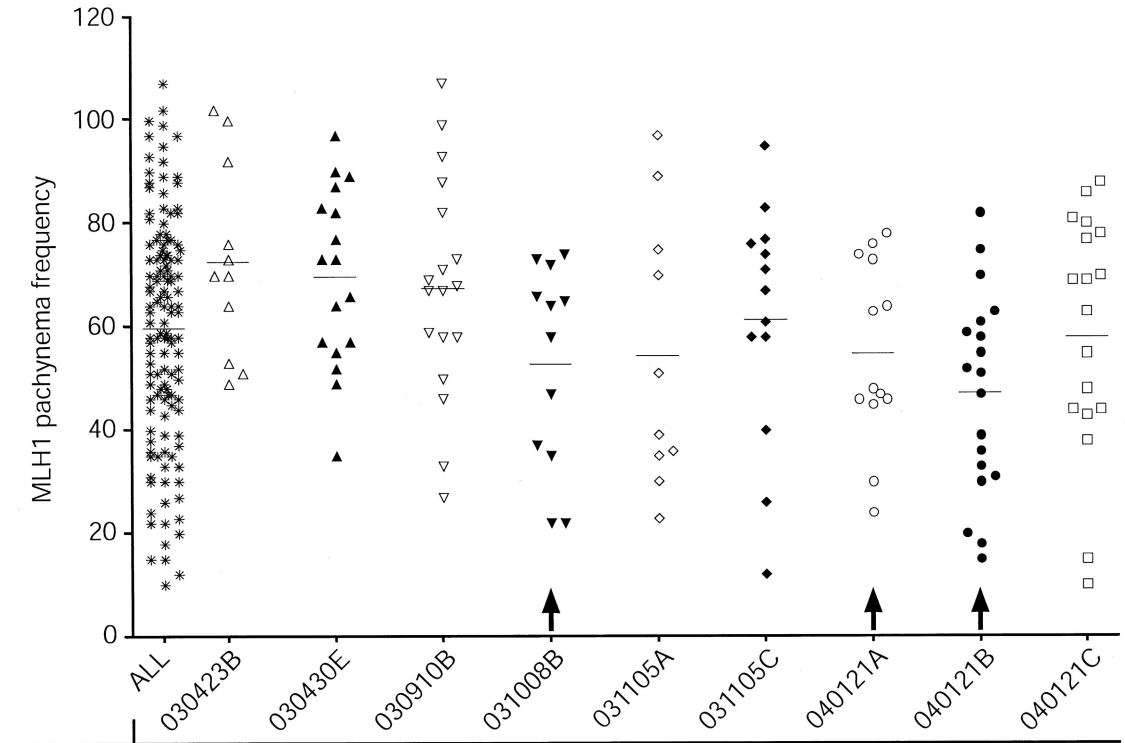

	030423B	030430E	030910B	031008B	031105A	031105C	040121A	040121B	040121C
030423B	-	-	-	-	-	-	-	-	-
030430E	n.s.	-	-	-	-	-	-	-	-
030910B	n.s.	n.s.	-	-	-	-	-	-	-
031008B	*P*<.05	*P*<.05	*P*<.05	-	-	-	-	-	-
031105A	n.s.	n.s.	n.s.	n.s.	-	-	-	-	-
031105C	n.s.	n.s.	n.s.	n.s.	n.s.	-	-	-	-
040121A	*P*<.05	*P*<.01	n.s.	n.s.	n.s.	n.s.	-	-	-
040121B	*P*<.001	*P*<.001	*P*<.005	n.s.	n.s.	n.s.	n.s.	-	-
040121C	n.s.	n.s.	n.s.	n.s.	n.s.	n.s.	n.s.	n.s.	-

Figure 7 MLH1 localization during pachynema in oocyte pools from individual fetal ovary samples. Each column represents oocytes from an individual fetal ovary pair (gestational age 17–24 wk). The "ALL" column represents MLH1 counts in the entire pool of ovaries. Results from unpaired *t* tests are given below each column. Certain oocyte pools have significantly lower MLH1 focus frequencies (*arrows*); n.s. = not significant.

association of MLH1-MLH3 with MSH4-MSH5 has been proposed as an important prerequisite for chromosome segregation (Hollingsworth et al. 1995; Hunter and Borts 1997; Winand et al. 1998; Kneitz et al. 2000; Santucci-Darmanin et al. 2000; Novak et al. 2001; Kolas and Cohen 2004; Snowden et al. 2004), and, therefore, the reduced ability of MLH1-MLH3 to associate with MSH4-MSH5 in certain oocytes might destabilize the complex at dHJs and, in turn, might jeopardize crossover fidelity.

Mice carrying homozygous mutations in *Mlh1* or *Mlh3* are sterile, as a result of a failure to maintain synapsis of chromosomes after pachynema (Baker et al. 1996; Edelmann et al. 1996; Lipkin et al. 2002). In both male and female mice, the absence of MLH1 and/or MLH3 does not affect synapsis or progression until pachynema. In contrast, *Msh4* and *Msh5* homozygous mutant animals exhibit failed and/or inappropriate synapsis, which results in meiotic failure prior to pachynema in both male and female $Msh4^{-/-}$ and $Msh5^{-/-}$ mice (de Vries et al. 1999; Edelmann et al. 1999; Kneitz et al. 2000). In $Mlh1^{-/-}$ and $Mlh3^{-/-}$ mice, on the other hand, meiocytes progress beyond pachynema, but, once the central element of the SC begins to disassemble during diplonema and homologs begin to repel each other, the crossover structures are no longer capable of keeping the chromosomes together until metaphase, which results in premature desynapsis. Despite a similar meiotic failure, however, the ultimate loss of germ cells is very different in males and females lacking these MutL homologs. In

Mlh1$^{-/-}$ and *Mlh3*$^{-/-}$ males, chromosomes desynapse almost completely, with <10% of crossovers remaining (Baker et al. 1996; Lipkin et al. 2002), and the cells enter apoptosis prior to or at metaphase (Eaker et al. 2002), which demonstrates that the onset of cell death is temporally distinct from the actual meiotic defect. Interestingly, the same meiotic defect in females results in a temporally distinct cellular response. In both *Mlh1*$^{-/-}$ and *Mlh3*$^{-/-}$ females, the chromosomes appear at prometaphase in largely univalent form and are thus unable to establish bipolar spindle attachments (Woods et al. 1999; Lipkin et al. 2002). This results, at least in *Mlh1*$^{-/-}$ females, in spindles that never become stabilized, with chromosomes dispersed nonuniformly throughout the spindle apparatus (Woods et al. 1999). Oocytes from *Mlh1*$^{-/-}$ females progress through metaphase, but the chromosomes mis-segregate between the oocyte and first polar body and, upon fertilization, fail to progress appropriately through the early cleavage stages of development (Edelmann et al. 1996; Woods et al. 1999; Lipkin et al. 2002). Thus, in males lacking MLH1-MLH3, we observe a failure of meiosis in the pachytene to diplotene stages of prophase I, with a consequent apoptotic switch at metaphase, whereas females lacking MLH1-MLH3 escape the metaphase apoptotic "checkpoint," and the oocytes attempt to progress through metaphase I. Together, these observations demonstrate that loss of MLH1-MLH3 in females is likely to reduce recombination rates to <10% of normal (extrapolating from the known residual recombination rate in MLH1-deficient males [Baker et al. 1996]), but without an associated checkpoint activation.

In general, the selection of reciprocal recombinant sites from the pool of DSBs follows some simple rules: at least one crossover is required per chromosome and the longer the chromosome, the more likely it is that there will be more than one crossover (van Veen and Hawley 2003). In the present study, the intervals between MLH1 foci were fitted to a gamma model, and an interference parameter was calculated. For all MLH1 intervals, the interference parameter was 3.11 (95% CI 2.84–3.40). Since a value of 1 would imply no interference, the computed value indicates that positive interference is acting to restrict and/or regulate MLH1 targeting to nascent crossovers. A minimum of 23–46 MLH1 foci, representing 1 or 2 meiotic nodules per chromosome, would be expected to ensure proper segregation at metaphase I in human oocytes by resulting in a level of at least 1 crossover per chromosome. Clearly, a large majority of the oocytes (~28%) observed in the present study fall below this optimal threshold, which suggests that these oocytes would be more susceptible to nondisjunction than those within the normal range.

Interestingly, oocyte populations from some ovaries display statistically lower MLH1 numbers (fig. 7), which suggests that recombination events are susceptible to genetic and/or environmental factors. This would suggest that some individuals might be more susceptible to aneuploidy-inducing events during embryogenesis than others. Alternatively, those oocytes that have too few (or perhaps too many) MLH1 foci might instead be eliminated during the wave of perinatal attrition that occurs in the ovary and that reduces the oocyte count from >7 million at 20 wk gestation to 1–2 million at birth (Tilly 2001). This possibility has been difficult to evaluate because of limited tissue availability, but it leads to an intriguing speculation that the oocytes lost during the neonatal attrition period may be predestined as a result of errors during prophase I. Such a "surveillance" mechanism might substitute for the less stringent metaphase checkpoint system in female meiosis and could be mediated through the interconnected oocyte cyst structure during embryogenesis, ensuring that the healthiest oocytes in a cyst would survive and would claim all the metabolic resources from the unhealthy oocytes within the cyst (Pepling and Spradling 2001). Such a mechanism, by reducing the oocyte pool from the outset, might also provide an explanation for human infertility issues such as premature ovarian failure.

One other possible explanation for the variable MLH1-MLH3 focus numbers is that this MutL homolog may appear later in prophase I than is possible to observe with our system. Pregnancy terminations are limited to the first 24 wk of gestation, and it is possible that many oocytes could acquire MLH1 in later stages of prophase I that cannot be seen at 24 wk. This possibility is unlikely, since many oocytes are found at later stages of pachynema and diplonema in these tissues; however, this option cannot be excluded entirely. Although our data do not favor any of these three options (later appearance of MLH1 or reduced MLH1 foci resulting in chiasmata frequency that in turn leads either to aneuploidy in postnatal oocytes or to increased risk of oocyte attrition at birth), they do support the idea that variability in MMR-driven events is responsible for producing a heterogeneous population of oocytes during the critical stages of meiotic prophase in human fetal oocytes. The fact that such variability clearly does not exist in human males or in male and female mice indicates a fundamental difference in meiotic progression in human females that correlates well with the higher incidence of aneuploidy in human oocytes.

In humans, an association has been found between aberrant recombination and the incidence of trisomic disorders (reviewed by Hassold and Hunt [2001]). Reduced recombination rates for chromosome 21 are associated with a higher incidence of Down syndrome (Warren et al. 1987; Sherman et al. 1991, 1994; Savage et al. 1998; Brown et al. 2000), as is altered distribution of recombination events (Hassold and Sherman 2000;

Hassold et al. 2000). Similar aberrant recombination events are associated with trisomies involving chromosomes 15, 16, and 18 (reviewed by Hassold and Sherman [2000]). In addition, Broman et al. (1998) have reported significant interindividual variation in recombination frequencies among women, independent of maternal age. These observations have led investigators to suggest that a "threshold" of adequate recombination exists for each chromosome that ensures correct disjunction at the first meiotic division (Brown et al. 2000), similar to the optimal threshold of MLH1-MLH3 foci that we have proposed in the present study. Although this relationship remains indirect, further exploration should shed light on the implications of these associations for human aneuploidy.

Acknowledgments

This work was supported by March of Dimes Birth Defects Foundation funding (grant 1-FY02-177 to P.E.C.) and by Albert Einstein College of Medicine start-up funding. We thank Nadine Kolas for insightful comments, technical expertise, and suggestions throughout the course of this work. We are also indebted to Dr. Terry Ashley of the Department of Genetics at Yale University School of Medicine for support and advice.

Electronic-Database Information

The URL for data presented herein is as follows:

Online Mendelian Inheritance in Man (OMIM), http://www.ncbi.nlm.nih.gov/Omim/ (for Sycp3, RAD51, RPA, MSH4, MSH5, MLH1, MLH3, H2AX, and *SPO11* clone)

References

Abdullah MF, Hoffmann ER, Cotton VE, Borts RH (2004) A role for the MutL homologue MLH2 in controlling heteroduplex formation and in regulating between two different crossover pathways in budding yeast. Cytogenet Genome Res 107:180–190

Allers T, Lichten M (2001) Intermediates of yeast meiotic recombination contain heteroduplex DNA. Mol Cell 8:225–231

Ashley T, Plug AW, Xu J, Solari AJ, Reddy G, Golub EI, Ward DC (1995) Dynamic changes in Rad51 distribution on chromatin during meiosis in male and female vertebrates. Chromosoma 104:19–28

Baker SM, Plug AW, Prolla TA, Bronner CE, Harris AC, Yao X, Christie DM, Monell C, Arnheim N, Bradley A, Ashley T, Liskay RM (1996) Involvement of mouse Mlh1 in DNA mismatch repair and meiotic crossing over. Nat Genet 13:336–342

Bannister LA, Schimenti JC (2004) Homologous recombinational repair proteins in mouse meiosis. Cytogenet Genome Res 107:191–200

Barlow AL, Benson FE, West SC, Hulten MA (1997) Distribution of the Rad51 recombinase in human and mouse spermatocytes. EMBO J 16:5207–5215

Barlow AL, Hulten MA (1998) Crossing over analysis at pachytene in man. Eur J Hum Genet 6:350–358

Bishop DK (1994) RecA homologs Dmc1 and Rad51 interact to form multiple nuclear complexes prior to meiotic chromosome synapsis. Cell 79:1081–1092

Bocker T, Barusevicius A, Snowden T, Rasio D, Guerrette S, Robbins D, Schmidt C, Burczak J, Croce CM, Copeland T, Kovatich AJ, Fishel R (1999) hMSH5: a human MutS homologue that forms a novel heterodimer with MSH4 and is expressed during spermatogenesis. Cancer Res 59:816–822

Borts RH, Chambers SR, Abdullah MF (2000) The many faces of mismatch repair in meiosis. Mutat Res 451:129–150

Broman KW, Murray JC, Sheffield VC, White RL, Weber JL (1998) Comprehensive human genetic maps: individual and sex-specific variation in recombination. Am J Hum Genet 63:861–869

Broman KW, Weber JL (2000) Characterization of human crossover interference. Am J Hum Genet 66:1911–1926

Brown AS, Feingold E, Broman KW, Sherman SL (2000) Genome-wide variation in recombination in female meiosis: a risk factor for non-disjunction of chromosome 21. Hum Mol Genet 9:515–523

Cohen PE, Pollard JW (2001) Regulation of meiotic recombination and prophase I progression in mammals. Bioessays 23:996–1009

de Vries SS, Baart EB, Dekker M, Siezen A, de Rooij DG, de Boer P, te Riele H (1999) Mouse MutS-like protein Msh5 is required for proper chromosome synapsis in male and female meiosis. Genes Dev 13:523–531

Eaker S, Cobb J, Pyle A, Handel MA (2002) Meiotic prophase abnormalities and metaphase cell death in MLH1-deficient mouse spermatocytes: insights into regulation of spermatogenic progress. Dev Biol 249:85–95

Edelmann W, Cohen PE, Kane M, Lau K, Morrow B, Bennett S, Umar A, Kunkel T, Cattoretti G, Chaganti R, Pollard JW, Kolodner RD, Kucherlapati R (1996) Meiotic pachytene arrest in MLH1-deficient mice. Cell 85:1125–1134

Edelmann W, Cohen PE, Kneitz B, Winand N, Lia M, Heyer J, Kolodner R, Pollard JW, Kucherlapati R (1999) Mammalian MutS homologue 5 is required for chromosome pairing in meiosis. Nat Genet 21:123–127

Hamer G, Roepers-Gajadien HL, van Duyn-Goedhart A, Gademan IS, Kal HB, van Buul PP, de Rooij DG (2003) DNA double-strand breaks and gamma-H2AX signaling in the testis. Biol Reprod 68:628–634

Hassold T, Hunt P (2001) To err (meiotically) is human: the genesis of human aneuploidy. Nat Rev Genet 2:280–291

Hassold T, Judis L, Chan ER, Schwartz S, Seftel A, Lynn A (2004) Cytological studies of meiotic recombination in human males. Cytogenet Genome Res 107:249–255

Hassold T, Sherman S (2000) Down syndrome: genetic recombination and the origin of the extra chromosome 21. Clin Genet 57:95–100

Hassold T, Sherman S, Hunt PA (2000) Counting cross-overs: characterizing meiotic recombination in mammals. Hum Mol Genet 9:2409–2419

Higgins JD, Armstrong SJ, Franklin FC, Jones GH (2004) The *Arabidopsis MutS* homolog *AtMSH4* functions at an early

step in recombination: evidence for two classes of recombination in *Arabidopsis*. Genes Dev 18:2557–2570
Hoffmann ER, Borts RH (2004) Meiotic recombination intermediates and mismatch repair proteins. Cytogenet Genome Res 107:232–248
Hoffmann ER, Shcherbakova PV, Kunkel TA, Borts RH (2003) MLH1 mutations differentially affect meiotic functions in *Saccharomyces cerevisiae*. Genetics 163:515–526
Hollingsworth NM, Ponte L, Halsey C (1995) MSH5, a novel MutS homolog, facilitates meiotic reciprocal recombination between homologs in Saccharomyces cerevisiae but not mismatch repair. Genes Dev 9:1728–1739
Hunter N, Borts RH (1997) Mlh1 is unique among mismatch repair proteins in its ability to promote crossing-over during meiosis. Genes Dev 11:1573–1582
Judis L, Chan ER, Schwartz S, Seftel A, Hassold T (2004) Meiosis I arrest and azoospermia in an infertile male explained by failure of formation of a component of the synaptonemal complex. Fertil Steril 81:205–209
Keeney S, Giroux CN, Kleckner N (1997) Meiosis-specific DNA double-strand breaks are catalyzed by Spo11, a member of a widely conserved protein family. Cell 88:375–384
Kelly KO, Dernburg AF, Stanfield GM, Villeneuve AM (2000) *Caenorhabditis elegans msh-5* is required for both normal and radiation-induced meiotic crossing over but not for completion of meiosis. Genetics 156:617–630
Kneitz B, Cohen PE, Avdievich E, Zhu L, Kane MF, Hou H Jr, Kolodner RD, Kucherlapati R, Pollard JW, Edelmann W (2000) MutS homolog 4 localization to meiotic chromosomes is required for chromosome pairing during meiosis in male and female mice. Genes Dev 14:1085–1097
Kolas NK, Cohen PE (2004) Novel and diverse functions of the DNA mismatch repair family in mammalian meiosis and recombination. Cytogenet Genome Res 107:216–231
Lipkin SM, Moens PB, Wang V, Lenzi ML, Shanmugarajah D, Gilgeous A, Thomas J, Cheng J, Touchman JW, Green ED, Schwartzberg P, Collins FS, Cohen PE (2002) Meiotic arrest and aneuploidy in MLH3-deficient mice. Nat Genet 31:385–390
Lynn A, Ashley T, Hassold T (2004) Variation in human meiotic recombination. Annu Rev Genomics Hum Genet 5:317–349
Mahadevaiah SK, Turner JM, Baudat F, Rogakou EP, de Boer P, Blanco-Rodriguez J, Jasin M, Keeney S, Bonner WM, Burgoyne PS (2001) Recombinational DNA double-strand breaks in mice precede synapsis. Nat Genet 27:271–276
Marcon E, Moens P (2003) MLH1p and MLH3p localize to precociously induced chiasmata of okadaic-acid-treated mouse spermatocytes. Genetics 165:2283–2287
Moens PB, Kolas NK, Tarsounas M, Marcon E, Cohen PE, Spyropoulos B (2002) The time course and chromosomal localization of recombination-related proteins at meiosis in the mouse are compatible with models that can resolve the early DNA-DNA interactions without reciprocal recombination. J Cell Sci 115:1611–1622
Novak JE, Ross-Macdonald PB, Roeder GS (2001) The budding yeast Msh4 protein functions in chromosome synapsis and the regulation of crossover distribution. Genetics 158: 1013–1025
Pepling ME, Spradling AC (2001) Mouse ovarian germ cell cysts undergo programmed breakdown to form primordial follicles. Dev Biol 234:339–351
Peters AH, Plug AW, van Vugt MJ, de Boer P (1997) A drying-down technique for the spreading of mammalian meiocytes from the male and female germline. Chromosome Res 5:66–68
Plug AW, Peters AH, Keegan KS, Hoekstra MF, de Boer P, Ashley T (1998) Changes in protein composition of meiotic nodules during mammalian meiosis. J Cell Sci 111:413–423
Plug AW, Xu J, Reddy G, Golub EI, Ashley T (1996) Presynaptic association of Rad51 protein with selected sites in meiotic chromatin. Proc Natl Acad Sci USA 93:5920–5924
Roig I, Liebe B, Egozcue J, Cabero L, Garcia M, Scherthan H (2004) Female-specific features of recombinational double-stranded DNA repair in relation to synapsis and telomere dynamics in human oocytes. Chromosoma 113:22–33
Romanienko PJ, Camerini-Otero RD (1999) Cloning, characterization, and localization of mouse and human *SPO11*. Genomics 61:156–169
Ross-Macdonald P, Roeder GS (1994) Mutation of a meiosis-specific MutS homolog decreases crossing over but not mismatch correction. Cell 79:1069–1080
Santucci-Darmanin S, Walpita D, Lespinasse F, Desnuelle C, Ashley T, Paquis-Flucklinger V (2000) MSH4 acts in conjunction with MLH1 during mammalian meiosis. FASEB J 14:1539–1547
Savage AR, Petersen MB, Pettay D, Taft L, Allran K, Freeman SB, Karadima G, Avramopoulos D, Torfs C, Mikkelsen M, Hassold TJ, Sherman SL (1998) Elucidating the mechanisms of paternal non-disjunction of chromosome 21 in humans. Hum Mol Genet 7:1221–1227
Sherman SL, Petersen MB, Freeman SB, Hersey J, Pettay D, Taft L, Frantzen M, Mikkelsen M, Hassold TJ (1994) Nondisjunction of chromosome 21 in maternal meiosis I: evidence for a maternal age-dependent mechanism involving reduced recombination. Hum Mol Genet 3:1529–1535
Sherman SL, Takaesu N, Freeman SB, Grantham M, Phillips C, Blackston RD, Jacobs PA, Cockwell AE, Freeman V, Uchida I, Mikkelsen M, Kurnit DM, Buraczynska M, Keats BJB, Hassold TJ (1991) Trisomy 21: association between reduced recombination and nondisjunction. Am J Hum Genet 49: 608–620
Snowden T, Acharya S, Butz C, Berardini M, Fishel R (2004) MSH4-MSH5 recognizes Holliday junctions and forms a meiosis-specific sliding clamp that embraces homologous chromosomes. Mol Cell 15:437–451
Tease C, Hartshorne GM, Hulten MA (2002) Patterns of meiotic recombination in human fetal oocytes. Am J Hum Genet 70:1469–1479
Tilly JL (2001) Commuting the death sentence: how oocytes strive to survive. Nat Rev Mol Cell Biol 2:838–848
van Veen JE, Hawley RS (2003) Meiosis: when even two is a crowd. Curr Biol 13:R831–R833
Wang TF, Kleckner N, Hunter N (1999) Functional specificity of MutL homologs in yeast: evidence for three Mlh1-based heterocomplexes with distinct roles during meiosis in recombination and mismatch correction. Proc Natl Acad Sci USA 96:13914–13919
Warren AC, Chakravarti A, Wong C, Slaugenhaupt SA, Hal-

loran SL, Watkins PC, Metaxotou C, Antonarakis SE (1987) Evidence for reduced recombination on the nondisjoined chromosomes 21 in Down syndrome. Science 237:652–654

Winand NJ, Panzer JA, Kolodner RD (1998) Cloning and characterization of the human and *Caenorhabditis elegans* homologs of the *Saccharomyces cerevisiae MSH5* gene. Genomics 53:69–80

Woods LM, Hodges CA, Baart E, Baker SM, Liskay RM, Hunt PA (1999) Chromosomal influence on meiotic spindle assembly: abnormal meiosis I in female Mlh1 mutant mice. J Cell Biol 145:1395–1406

Yuan L, Liu JG, Hoja MR, Wilbertz J, Nordqvist K, Hoog C (2002) Female germ cell aneuploidy and embryo death in mice lacking the meiosis-specific protein SCP3. Science 296: 1115–1118

Yuan L, Liu JG, Zhao J, Brundell E, Daneholt B, Hoog C (2000) The murine *SCP3* gene is required for synaptonemal complex assembly, chromosome synapsis, and male fertility. Mol Cell 5:73–83

Zalevsky J, MacQueen AJ, Duffy JB, Kemphues KJ, Villeneuve AM (1999) Crossing over during *Caenorhabditis elegans* meiosis requires a conserved MutS-based pathway that is partially dispensable in budding yeast. Genetics 153:1271–1283